Hindawi
Mathematical Problems in Engineering
Volume 2022, Article ID 3509721, 17 pages
https://doi.org/10.1155/2022/3509721

Research Article

Three-Dimensional Fluctuating Flow of a Second-Grade Fluid along an Infinite Horizontal Plate with Periodic Suction

Mehwish Zafar,[1] **Muhammad Afzal Rana**,[1] **and Atifa Latif**[1,2]

[1]*Department of Mathematics and Statistics, Riphah International University, Sector I-14, Islamabad 44000, Pakistan*
[2]*Department of Mathematics, GC University Faisalabad, Faisalabad, Pakistan*

Correspondence should be addressed to Muhammad Afzal Rana; mafzalrana@gmail.com and Atifa Latif; aatifalatif@gmail.com

Received 10 June 2022; Revised 31 August 2022; Accepted 3 October 2022; Published 29 October 2022

Academic Editor: Amer Rasheed

Laminar flow control plays a vital role in reducing drag resulting enhancement in the vehicle power by a significant amount. Theoretical and experimental studies have proven that the transition from laminar to turbulent flow (causing the drag coefficient to enhance) may be delayed/prevented by the suction of the fluid from the boundary layer to the wall. The purpose of this work is to study the effects of periodic suction on the unsteady 3-dimensional fluctuating flow of a second grade incompressible fluid flowing laminarly over a horizontal porous infinite plate. The plate is subjected to a sinusoidal transverse suction velocity while the free stream velocity oscillates in time about a constant mean. The flow turns out to be 3-dimensional because of transverse direction of the periodic suction velocity. By the series expansion method, analytic expressions for transient velocity, skin friction components, and pressure are attained. Impact of nondimensional parameters evolving in the mathematical model of the problem on these physical quantities are visualized graphically and discussed analytically. The velocity component u is found to be rising with a growth in suction parameter α. The pressure is noted to be growing with a growth in Reynolds number Re. Further, due to suction at the plate and transient free stream velocity, the pressure increases near the plate and then reaches to a steady value far-off the plate. The skin friction along the main flow is noticed to be decreasing with the rise in α for $0.5 \leq Re \leq 1.4$, however, an exponential rise is observed for $Re > 1.4$. The skin friction along the cross flow is noted to be enhancing for the rising values of suction parameter and elastic parameter. The present results have excellent agreement with previous published results in the limiting sense. This study is beneficial in designing and manufacturing laminar flow control system to enhance the vehicle power requirement.

1. Introduction

Studies are in progress to develop a laminar control system for the purpose of tumbling vehicle power requirements [1]. It has been proved experimentally and theoretically that the laminarization of the boundary layer over a profile lessens the drag resulting enhancement in the vehicle power requirement by a very substantial amount. For the sake of artificially controlling the boundary layer, many methods have been developed since World War II [1]. Theoretical and experimental studies have proven that the transition from laminar to turbulent flow (causing the drag coefficient to enhance) may be delayed/prevented by the suction of the fluid from the boundary layer to the wall. Geometry and configuration of the slits through which the suction takes place is very important and has been deliberated broadly by various scholars. Holes of numerous sizes and slots have received extensive consideration. There is an impervious segment between the suction openings for all configurations, and it is hypothetically apposite to imagine such an area with openings as a region of changing continuous suction. The transverse sinusoidal suction velocity approach is one of the possible suction distributions. This work is oriented with the behavior of such a sinusoidally changing suction distribution over a surface and its impact on the flow.

The oscillatory flows are ever momentous from the technological point of view and hence possess various real-world applications. Oscillatory unsteady flows, therefore,

play a vital role in aerospace technology, chemical engineering, and turbo machinery. Lighthill [2] initiated the study of such flows in 1954 and presented the free stream oscillations effects on an incompressible viscous fluid flow over an infinite plane. In 1955, Stuart [3] extended further this work for an oscillatory 2-dimensional laminar flow over an infinite porous plane with constant suction. It was observed that the flow in the neighbor of the plate is reversed constructing the boundary layer to detach from it. Further, in 1966, Messiha [4] analyzed oscillatory two-dimensional flow when suction depending on time is subjected to the plane. Soundalgekar [5] investigated the effects of free convection on the flow past an infinite vertical oscillatory plate with the wall temperature in 1979. Raptis [6], in 1985, explored the unsteady flow problem through a porous medium circumscribed by a porous infinite plane subjected to a temperature (variable) but on a constant suction. Singh and Rana [7] performed study of the heat transfer and a viscous fluid flow through a porous medium circumscribed by a plane at constant temperature and presented effects of periodic suction velocity on the heat transfer in 1992. Singh [8] analyzed an incompressible viscous fluid flow through a porous medium circumscribed by a porous infinite plane in the presence of periodic suction with free stream velocity oscillating with respect to time about a nonzero constant mean in 1992. Considerable prevention of separation in the porous medium was noted. Later on, in 1993, Helmy [9] explored the electrically conducting fluid flow across an infinite plate wall with variable suction. In 2006, Guria and Jana [10] analyzed Couette unsteady flow of an incompressible viscous fluid when the upper plate (moving uniformly) is subjected to injection (uniform) while the lower plate (stationary) is subjected to a periodic suction. Decrease in flow velocity (main) with an increase in frequency parameter was noted. However, a rise in cross flow velocity magnitude with a grow in frequency parameter was presented. In 2010, Ahmed [11] studied unsteady three-dimensional flow of an incompressible viscous fluid past a porous vertical infinite plate with heat transfer and viscous dissipation. Workers [12–14] scrutinized transient 3-dimensional flow of viscous fluid under different physical conditions. Gersten and Gross [15] examined heat flow along a plane wall with periodic suction under the asymptotic flow conditions for downstream and determined the wall shear stress components. The researchers [16–18] analyzed technically the fluctuating flow of some Newtonian fluids through porous mediums with different rotating geometries, and they established adequate results. Mabood et al. [19] examined the effects of thermal radiation and melting heat transfer in a stagnation point flow towards a shrinking/stretching surface. Numerical solutions based on the Runge–Kutta fourth-fifth order method for the resulting nonlinear problems were obtained.

All above mentioned studies have been performed for Newtonian fluids. However, majority of fluids used in industries are non-Newtonian ones. Therefore, without the study of non-Newtonian fluids, the problems associated with industries issues remain unaddressed. Shoaib et al. [20] dissected steady 3-D flow of a second grade fluid over an infinite horizontal plane subjected to a sinusoidal transverse suction velocity. They found the existence of backflow. Rana and Latif [21] presented 3-dimensional free convective second-grade fluid flow with periodic permeability and heat transfer through a porous medium. They noted a rise in pressure because of fluid thickening. Bhatti et al. [22] analyzed electro-osmotic flow of Jeffery fluid in the presence of small particles moving in the sinusoidal form in a Darcy–Brinkman–Forchheimer medium and transversely applied magnetic field. Riaz et al. [23] presented the exact solutions of non-Newtonian multiphase fluid flow through peristaltic pumping characteristics in an annulus having complaint walls and applied magnetic field. It was concluded that applied magnetic field decreases the velocity of both the fluid and the particles flow. Gireesha et al. [24] analyzed the effect of nanoparticles on a steady MHD flow and heat and mass transfer of Eyring–Powell fluid in two lateral directions over a convectively heated stretching sheet. Similarity transformations were employed to reduce the governing partial differential equations into a set of nonlinear ordinary differential equations which were solved numerically using the fourth-fifth order Runge–Kutta–Fehlberg method with the shooting technique. Mahanthesh et al. [25] scrutinized numerically the combined effects of nonlinear thermal convection and radiation in 3D boundary layer flow of Maxwell nanofluid over a stretching sheet. The solutions were computed via the homotopy procedure. It was noted that the nanoparticle volume fraction and temperature profiles are stronger for the case of solar radiation in comparison with the problem without radiation. Shafiq et al. [26] examined the second grade bioconvective nanofluid flow with the buoyancy effect and chemical reaction. The Brownian motion and thermophoretic mechanisms along with Newtonian heating were also considered. Mass flux was found to be enhancing function of both Brownian diffusion parameter and Lewis number. Mabood et al. [27] studied rheological aspects on the micropolar fluid model by simulating the reactive flow from a continuously moving flat plate. The model was developed employing Brownian motion, thermophoretic diffusion, and chemically reactive species. It was found that the presence of thermophoresis and Brownian motion is more effective to improve the heat transportation phenomenon. Shamshuddin et al. [28] scrutinized the magnetized flow of Casson nanofluid past a Riga surface with nonlinear radiative, uneven heat sink/source, thermophoretic movement, and chemical reaction. The analysis revealed that an increment in the Casson term causes a rise in the temperature profile for CuO and MgO nanofluid and dominant behavior is noted in case of CuO nanofluid on comparing with MgO nanofluid.

Above mentioned studies were carried out for steady flows of non-Newtonian fluids; however, oscillatory unsteady flows play a vital role in aerospace technology, turbo machinery, and chemical engineering. The objective of this study is to analyze periodic suction velocity effect on the 3-D flow of a second-grade incompressible fluid flowing laminarly over a horizontal infinite plane with a free stream oscillatory velocity. To the best of authors' information, no such investigation has been carried out. Basically, laminar

flow control performs a vital role in reducing drag resulting enhancement in the vehicle power by a significant amount; therefore, the present study is relevant to various engineering sciences applications, particularly, relevant to aeronautical engineering.

2. Mathematical Formulation

Consider an unsteady flow of a second grade incompressible fluid along an infinite porous plate lying horizontally on the x^*z^* – plane with x^* – axis along the plate, being the direction of the flow. The y^* – axis which is directed into the fluid is along normal to the plate. All fluid physical quantities are not dependent of x^* due to the plate infinite length in x^* – direction [11, 15]. The flow, however, ruins 3-D because of the transverse sinusoidal suction velocity [11, 15]:

$$v^*\left(z^*\right) = V_0\left(1 + \epsilon\cos\pi\frac{z^*}{l}\right), \tag{1}$$

where $(V_0 < 0)$ is suction velocity, l is the wave length of the suction distribution, and ϵ $(\ll 1)$ is the amplitude of the suction variation.

The continuity equation and momentum equation respectively governing the fluid flow are

$$\nabla.\overrightarrow{V} = 0, \tag{2}$$

$$\rho\frac{\mathrm{d}\overrightarrow{V}}{\mathrm{d}t} = \nabla.\widetilde{\tau}, \tag{3}$$

where

$$\overrightarrow{V} = [u^*\left(y^*, z^*, t^*\right), v^*\left(y^*, z^*, t^*\right), w^*\left(y^*, z^*, t^*\right)], \tag{4}$$

is velocity field, and the Cauchy stress tensor $\widetilde{\tau}$ for the second grade fluid model [29–31] is

$$\widetilde{\tau} = -p\widetilde{I} + \mu\widetilde{A}_1 + \alpha_1\widetilde{A}_2 + \alpha_2\widetilde{A}_1^2, \tag{5}$$

while Rivlin–Ericksen tensors, $\widetilde{A}_1$ and $\widetilde{A}_2$, are

$$\left.\begin{aligned}\widetilde{A}_1 &= (grad\overrightarrow{V})^T + grad\overrightarrow{V},\\ \widetilde{A}_2 &= (grad\overrightarrow{V})^T\widetilde{A}_1 + \widetilde{A}_1(grad\overrightarrow{V}) + \frac{\mathrm{d}\widetilde{A}_1}{\mathrm{d}t}.\end{aligned}\right\} \tag{6}$$

For the model (5) to meet the assumption that the specific Helmholtz free energy is a minimum in equilibrium and to be well-matched with the thermodynamics in the sense that all motions meet the Clausius–Duhem inequality [31], then

$$\alpha_1 \geq 0, \mu \geq 0, \alpha_1 + \alpha_2 = 0. \tag{7}$$

The equations (2) and (3) in view of Equations (4)–(7) yield

$$\frac{\partial v^*}{\partial y^*} + \frac{\partial w^*}{\partial z^*} = 0, \tag{8}$$

$$\left.\begin{aligned}&\rho\frac{\partial u^*}{\partial t^*} + \rho\left(v^*\frac{\partial u^*}{\partial y^*} + w^*\frac{\partial u^*}{\partial z^*}\right) = \rho\frac{\partial U^*}{\partial t^*} + \mu\left(\frac{\partial^2 u^*}{\partial y^{*2}} + \frac{\partial^2 u^*}{\partial z^{*2}}\right)\\ &+\alpha_1\left(v^*\frac{\partial^3 u^*}{\partial y^{*3}} + w\frac{\partial^3 u^*}{\partial z^*\partial y^{*2}} + v^*\frac{\partial^3 u^*}{\partial y^*\partial z^{*2}} + w^*\frac{\partial^3 u^*}{\partial z^{*3}}\right),\end{aligned}\right\} \tag{9}$$

$$\begin{aligned}&\rho\frac{\partial v^*}{\partial t^*} + \rho\left(v^*\frac{\partial v^*}{\partial y^*} + w^*\frac{\partial v^*}{\partial z^*}\right) = -\frac{\partial p^*}{\partial y^*} + \mu\left(\frac{\partial^2 v^*}{\partial y^{*2}} + \frac{\partial^2 v^*}{\partial z^{*2}}\right)\\ &+\alpha_1\left\{\begin{array}{l} v^*\dfrac{\partial^3 v^*}{\partial y^{*3}} + w\dfrac{\partial^3 v^*}{\partial z^*\partial y^{*2}} + v^*\dfrac{\partial^3 v^*}{\partial y^*\partial z^{*2}} + w^*\dfrac{\partial^3 v^*}{\partial z^{*3}}\\ +5\dfrac{\partial v^*}{\partial y^*}\dfrac{\partial^2 v^*}{\partial y^{2*}} + 2\dfrac{\partial u^*\partial^2 u^*}{\partial y^*\partial y^{2*}} + 2\dfrac{\partial w^*\partial^2 w^*}{\partial y^*\partial y^{2*}} + \dfrac{\partial v^*\partial^2 w^*}{\partial z^*\partial y^{2*}}\\ +\dfrac{\partial u^*}{\partial z^*}\dfrac{\partial^2 u^*}{\partial z^*\partial y^*} + \dfrac{\partial u^*}{\partial y^*}\dfrac{\partial^2 u^*}{\partial z^{2*}} + \dfrac{\partial v^*}{\partial y^*}\dfrac{\partial^2 v^*}{\partial z^{2*}} + \dfrac{\partial v^*}{\partial z^*}\dfrac{\partial^2 v^*}{\partial z^*\partial y}\end{array}\right\},\end{aligned} \tag{10}$$

$$\rho\frac{\partial \mathrm{w}^*}{\partial t^*}+\rho\left(v^*\frac{\partial \mathrm{w}^*}{\partial y^*}+w^*\frac{\partial \mathrm{w}^*}{\partial z^*}\right)=-\frac{\partial p^*}{\partial z^*}+\mu\left(\frac{\partial^2 \mathrm{w}^*}{\partial y^{*2}}+\frac{\partial^2 \mathrm{w}^*}{\partial z^{*2}}\right)$$
$$+\alpha_1\left\{\begin{array}{c} v^*\dfrac{\partial^3 \mathrm{w}^*}{\partial y^{*3}}+w^*\dfrac{\partial^3 \mathrm{w}^*}{\partial z^*\partial y^{*2}}+v^*\dfrac{\partial^3 \mathrm{w}^*}{\partial z^*\partial y^{*2}}+w^*\dfrac{\partial^3 \mathrm{w}^*}{\partial z^{*3}} \\ +\dfrac{\partial \mathrm{w}^*}{\partial y^*}\dfrac{\partial^2 \mathrm{w}^*}{\partial y^{*2}\partial z^*}+\dfrac{\partial u^*\partial^2 u^*}{\partial y^*\partial y^{*2}\partial z^*}+5\dfrac{\partial w^*\partial^2 w^*}{\partial z^*\partial z^{*2}}+\dfrac{\partial w^*\partial^2 v^*}{\partial y^*\partial z^{*2}} \\ +2\dfrac{\partial u^*\partial^2 u^*}{\partial z^*\partial z^{2*}}+2\dfrac{\partial v^*\partial^2 v^*}{\partial z^*\partial z^{2*}}+\dfrac{\partial u^*\partial^2 u^*}{\partial z^*\partial z^{2*}}+\dfrac{\partial w^*\partial^2 w^*}{\partial z^*\partial y^{*2}} \end{array}\right\}. \tag{11}$$

The appropriate boundary conditions [11] are

$$\left.\begin{array}{l} u^*=0, v^*=V_0\left(1+\epsilon\ \cos\pi\dfrac{z^*}{l}\right), w^*=0 \text{ at } y^*=0, \\ u^*=U^*\left(t^*\right)=U_0\left(1+\epsilon e^{\mathrm{in}^* t^*}\right), v^*=V_0, w^*=0, p^*=p_\infty^* \text{ at } y^*\longrightarrow\infty, \end{array}\right\}, \tag{12}$$

where n^* is frequency of free stream oscillation and t^* denotes time.

3. Dimensionless Equations

Introducing the nondimensional variables,

$$\left.\begin{array}{l} y=\dfrac{y^*}{l}, z=\dfrac{z^*}{l}, u=\dfrac{u^*}{U_0}, v=\dfrac{v^*}{U_0}, w=\dfrac{w^*}{U_0}, U=\dfrac{U^*}{U_0}, \\ t=n^*t^*, n=\dfrac{n^*l^2}{\vartheta}, p=\dfrac{p^*}{\rho U_0^2}, p_\infty=\dfrac{p_\infty^*}{\rho U_0^2}, \end{array}\right\}, \tag{13}$$

$$\left.\begin{array}{l} \alpha=\dfrac{V_0}{U_0}\ (\text{Suction parameter}), \\ Re=\dfrac{U_0 l}{\vartheta}\ (\text{Reynolds number}), \\ K=\dfrac{\alpha_1}{\rho l^2}\ (\text{Elastic parameter}), \end{array}\right\}, \tag{14}$$

then the equations (8)–(11) become

$$\frac{\partial v}{\partial y}+\frac{\partial w}{\partial z}=0, \tag{15}$$

$$\frac{n}{Re}\frac{\partial u}{\partial t}+\left(v\frac{\partial u}{\partial y}+w\frac{\partial u}{\partial z}\right)=\frac{n}{Re}\frac{\partial U}{\partial t}+\frac{1}{Re}\left(\frac{\partial^2 u}{\partial y^2}+\frac{\partial^2 u}{\partial z^2}\right)+K\left\{\begin{array}{l} v\dfrac{\partial^3 u}{\partial y^3}+w\dfrac{\partial^3 u}{\partial z\,\partial y^2}+ \\ v\dfrac{\partial^3 u}{\partial y\,\partial z^2}+w\dfrac{\partial^3 u}{\partial z^3} \end{array}\right\}, \tag{16}$$

$$\frac{n}{Re}\frac{\partial v}{\partial t}+\left(v\frac{\partial v}{\partial y}+w\frac{\partial v}{\partial z}\right)=-\frac{\partial p}{\partial y}+\frac{1}{Re}\left\{\frac{\partial^2 v}{\partial y^2}+\frac{\partial^2 v}{\partial z^2}\right\}+K\left\{\begin{array}{l} v\dfrac{\partial^3 v}{\partial y^3}+w\dfrac{\partial^3 v}{\partial z\,\partial y^2}+v\dfrac{\partial^3 v}{\partial y\,\partial z^2}+ \\ w\dfrac{\partial^3 v}{\partial z^3}+5\dfrac{\partial v}{\partial y}\dfrac{\partial^2 v}{\partial y^2}+2\dfrac{\partial u}{\partial y}\dfrac{\partial^2 u}{\partial y^2}+ \\ 2\dfrac{\partial w}{\partial y}\dfrac{\partial^2 w}{\partial y^2}+\dfrac{\partial u}{\partial z}\dfrac{\partial^2 u}{\partial z\,\partial y}+\dfrac{\partial v}{\partial z}\dfrac{\partial^2 w}{\partial y^2}+ \\ \dfrac{\partial u}{\partial y}\dfrac{\partial^2 u}{\partial z^2}+\dfrac{\partial v}{\partial y}\dfrac{\partial^2 v}{\partial z^2}+\dfrac{\partial v}{\partial z}\dfrac{\partial^2 v}{\partial z\,\partial y} \end{array}\right\}, \tag{17}$$

$$\frac{n}{Re}\frac{\partial w}{\partial t}+\left(v\frac{\partial w}{\partial y}+w\frac{\partial w}{\partial z}\right)=-\frac{\partial p}{\partial z}+\frac{1}{Re}\left\{\frac{\partial^2 w}{\partial y^2}+\frac{\partial^2 w}{\partial z^2}\right\}+K\left\{\begin{array}{l} v\dfrac{\partial^3 w}{\partial y^3}+w\dfrac{\partial^3 w}{\partial z\,\partial y^2}+v\dfrac{\partial^3 w}{\partial y\,\partial z^2}+ \\ w\dfrac{\partial^3 w}{\partial z^3}+5\dfrac{\partial w}{\partial z}\dfrac{\partial^2 w}{\partial z^2}+2\dfrac{\partial u}{\partial z}\dfrac{\partial^2 u}{\partial z^2}+ \\ \dfrac{\partial w}{\partial y}\dfrac{\partial^2 w}{\partial y\,\partial z}+\dfrac{\partial w}{\partial z}\dfrac{\partial^2 w}{\partial y^2}+2\dfrac{\partial v}{\partial z}\dfrac{\partial^2 v}{\partial z^2}+ \\ \dfrac{\partial u}{\partial z}\dfrac{\partial^2 u}{\partial y^2}+\dfrac{\partial u}{\partial y}\dfrac{\partial^2 u}{\partial y\,\partial z}+\dfrac{\partial w}{\partial y}\dfrac{\partial^2 v}{\partial z^2} \end{array}\right\}. \tag{18}$$

The corresponding boundary conditions (12) reduce to

$$\left.\begin{array}{l} u=0, v=\alpha(1+\epsilon\,\cos\,\pi z), w=0 \text{ at } y=0, \\ u=\left(1+\epsilon e^{\text{int}}\right), v=\alpha, w=0, p=p_\infty \text{ as } y\longrightarrow\infty. \end{array}\right\}. \tag{19}$$

It is wealth mentioning that the set of nonlinear partial differential equations (16)–(18) reduce to momentum equations of [11] for non-Newtonian parameter $K\longrightarrow 0$ and momentum equations of [21] under identical physical conditions.

4. Solution

As the amplitude $\epsilon\ll 1$, we take up solutions for the equations (15)–(18) in the vicinity of the plate in the form:

$$F(y,z,t)=F_0(y)+\epsilon F_1(y,z,t)+\epsilon^2 F_2(y,z,t)+\cdots, \tag{20}$$

where F stands for any u, v, w, and p.

For $\epsilon\epsilon=0$, the problem becomes the 2-dimensional steady flow having constant suction at the plate. Plugging in the series (20) into equations (15)–(19), the zeroth order equations in ϵ are as follows and equation (15) yields

$$\frac{dv_0}{dy}=0\Rightarrow v_0=\text{constant}. \tag{21}$$

The boundary condition $v_0(0)=\alpha\Rightarrow v_0=\alpha$.

From equation (16), the zeroth order equation is

$$v_0\frac{du_0}{dy}=\frac{1}{Re}\frac{d^2u_0}{dy^2}+Kv_0\frac{d^3u_0}{dy^3}. \tag{22}$$

In view of $v_0=\alpha$ and the boundary conditions (19), the zeroth order boundary value problem becomes

$$K\alpha\frac{d^3u_0}{dy^3}+\frac{1}{Re}\frac{d^2u_0}{dy^2}-\alpha\frac{du_0}{dy}=0,\quad \left.\begin{array}{ll} u_0=0 & \text{at } y=0, \\ u_0=1 & \text{at } y\longrightarrow\infty. \end{array}\right\}. \tag{23}$$

The differential (23) has order higher than the available boundary conditions as a result of elastic parameter K. For unique solution of the differential equation, three boundary conditions are required. To resolve this issue, we expand solution u_0 in the power series of $K(\ll 1)$ such that

$$u_0=u_{00}+Ku_{01}+O\left(K^2\right). \tag{24}$$

Employing equation (24) in equation (23) and comparing like terms in $O(K^0)$ and $O(K)$ on both sides to get the zeroth order and first order boundary value problems is given by

$$\left.\begin{array}{l} \dfrac{d^2u_{00}}{dy^2}-\alpha Re\dfrac{du_{00}}{dy}=0, \\ u_{00}(0)=0,\quad u_{00}(\infty)=1 \end{array}\right\}, \tag{25}$$

and

$$\left.\begin{array}{l} \alpha Re\dfrac{d^3u_{00}}{dy^3}+\dfrac{d^2u_{01}}{dy^2}-\alpha Re\dfrac{du_{01}}{dy}=0, \\ u_{01}(0)=0,\quad u_{01}(\infty)=0 \end{array}\right\}. \tag{26}$$

Now, solving the boundary value problem (25), we get

$$u_{00}(y) = 1 - e^{\alpha Rey}. \tag{27}$$

In view of solution (27), the boundary value problem (26) yields

$$\frac{d^2u_{01}}{dy^2} - \alpha Re\frac{du_{01}}{dy} = (\alpha Re)^4 e^{\alpha Rey}, \quad u_{01}(0) = 0, \quad u_{01}(\infty) = 0\}. \tag{28}$$

Its solution is

$$u_{01}(y) = (\alpha Re)^3 ye^{\alpha Rey}. \tag{29}$$

Hence, we get

$$u_0(y) = 1 - e^{\alpha Rey} + K(\alpha Re)^3 ye^{\alpha Rey}. \tag{30}$$

When $\in \neq 0$, the substitution of equation (20) for u, v, w into the equations (15)–(19) and comparison of the coefficients of $\in$ yields partial differential equations that is given by

$$\frac{\partial v_1}{\partial y} + \frac{\partial w_1}{\partial z} = 0, \tag{31}$$

$$\frac{n}{Re}\frac{\partial u_1}{\partial t} + v_1\frac{\partial u_0}{\partial y} + \alpha\frac{\partial u_1}{\partial y} = \frac{1}{Re}\left(\frac{\partial^2 u_1}{\partial y^2} + \frac{\partial^2 u_1}{\partial z^2}\right) + \frac{in^2}{Re}e^{int} + K\left(\alpha\frac{\partial^3 u_1}{\partial y^3} + \alpha\frac{\partial^3 u_1}{\partial y\,\partial z^2} + v_1\frac{\partial^3 u_1}{\partial y^3}\right), \tag{32}$$

$$\frac{n}{Re}\frac{\partial v_1}{\partial t} + \alpha\frac{\partial v_1}{\partial y} = -\frac{\partial p_1}{\partial y} + \frac{1}{Re}\left(\frac{\partial^2 v_1}{\partial y^2} + \frac{\partial^2 v_1}{\partial z^2}\right) + K\alpha\left(\frac{\partial^3 v_1}{\partial y^3} + \frac{\partial^3 v_1}{\partial y\,\partial z^2}\right), \tag{33}$$

$$\frac{n}{Re}\frac{\partial w_1}{\partial t} + \alpha\frac{\partial w_1}{\partial y} = -\frac{\partial p_1}{\partial z} + \frac{1}{Re}\left(\frac{\partial^2 w_1}{\partial y^2} + \frac{\partial^2 w_1}{\partial z^2}\right) + K\alpha\left(\frac{\partial^3 w_1}{\partial y^3} + \frac{\partial^3 w_1}{\partial y\,\partial z^2}\right). \tag{34}$$

Likewise, boundary conditions are

$$\left.\begin{aligned} &u_1 = 0, v_1 = \alpha\cos\pi z, w_1 = 0 \text{ at } y = 0,\\ &u_1 = e^{int}, v_1 = 0, w_1 = 0, p_1 = 0 \text{ as } y \longrightarrow \infty. \end{aligned}\right\}. \tag{35}$$

The set of differential equations (31)–(34) describe the unsteady three-dimensional flow. The equation (32) governs the main flow while equations (31), (33), and (34) govern the cross flow.

5. Cross Flow, Main Flow Solutions, and Pressure

In order to solve the boundary value problems (32)–(35), we consider the solutions for u_1, v_1, w_1, p_1 in the form of following complex notations whose real parts have physical consequence:

$$u_1(y,z,t) = v_{11}(y)e^{int} + v_{12}(y)\cos\pi z, \tag{36}$$

$$v_1(y,z,t) = v_{11}(y)e^{int} + v_{12}(y)\cos\pi z, \tag{37}$$

$$w_1(y,z,t) = -\left(zv'_{11}(y)e^{int} + \frac{1}{\pi}v'_{12}(y)\sin\pi z\right), \tag{38}$$

$$p_1(y,z,t) = p_{11}(y)e^{int} + p_{12}(y)\cos\pi z. \tag{39}$$

We note that the velocity components (37) and (38) identically satisfy the continuity equation (31). Moreover, prime denotes differentiation with respect to y. Setting these equations into equations (32)–(35) and solving the resulting partial differential equations to get the solutions for u_1, v_1, w_1, and p_1 given by

$$u_1(y,z,t) = \left(1 - e^{-\beta y}\right)e^{int} + \left[\frac{\alpha^2 Re^2}{\pi - \lambda}\left[\left(\frac{\lambda}{\pi\alpha Re} - \frac{\pi}{2\lambda\alpha Re}\right)e^{-\lambda y} + \frac{\pi}{2\lambda\alpha Re}e^{-(\lambda - \alpha Re)y} - \frac{\lambda}{\pi\alpha Re}e^{-(\pi - \alpha Re)y}\right] + K\left[\begin{array}{c} Fe^{-\lambda y} + (A - C)e^{-(\lambda - \alpha Re)y} + \\ (D - B + Ey)e^{-(\pi - \alpha Re)y} - 2Eye^{-(\lambda - \alpha Re)y} \end{array}\right]\right]\cos\pi z, \tag{40}$$

$$v_1(y,z,t) = \frac{\alpha}{\pi - \lambda}\left(\pi e^{-\lambda y} - \lambda e^{-\pi y}\right)\cos\pi z, \tag{41}$$

$$w_1(y,z,t) = \left(\frac{\alpha\lambda}{\pi - \lambda}\left(e^{-\lambda y} - e^{-\pi y}\right)\right)\sin\pi z, \tag{42}$$

$$p_1(y,z,t) = \frac{\alpha\lambda}{Re\pi(\pi-\lambda)}\left(K\alpha Re\lambda\left(\lambda^2-\pi^2\right)e^{-\lambda y} + \frac{\alpha^2\lambda}{\pi-\lambda}e^{-\pi y}\right)\cos\,\pi z, \tag{43}$$

where

$$\begin{aligned}
\lambda &= -\frac{\alpha Re}{2} + \sqrt{\left(\frac{\alpha Re}{2}\right)^2 + \pi^2},\\
\beta &= -\frac{\alpha Re}{2} + \sqrt{\left(\frac{\alpha Re}{2}\right)^2 + \mathrm{in}^2},\\
A &= \frac{\left((\alpha Re)^4\pi\right)/(\pi-\lambda) + (\alpha Re)^3\pi(\alpha Re-\lambda)\left(\pi^2-(\alpha Re-\lambda)^2\right)/(\pi-\lambda)2\lambda\alpha Re}{(\lambda-\alpha Re)^2 - \alpha Re(\alpha Re-\lambda) - \pi^2},\\
B &= \frac{\left((\alpha Re)^4\pi\right)/(\pi-\lambda) + (\alpha Re)^3\lambda(\alpha Re-\pi)\left((\alpha Re-\pi)^2-\pi^2\right)/(\pi-\lambda)\alpha Re\pi}{(\pi-\alpha Re)^2 - \alpha Re(\alpha Re-\pi) - \pi^2},\\
C &= \frac{\pi(\alpha Re)^5(\alpha Re-2\lambda)}{\pi-\lambda},\\
D &= \frac{\lambda(\alpha Re)^5(\alpha Re-2\pi)}{\pi-\lambda},\\
E &= \frac{\pi\lambda(\alpha Re)^6}{\pi-\lambda},\\
F &= -A+B+C-D.
\end{aligned} \tag{44}$$

In view of equations (30) and (40), we get

$$\begin{aligned}
u(y,z,t) = 1 - e^{\alpha Rey} + Ky(\alpha Re)^3 e^{\alpha Rey} + \epsilon\left[\left(1-e^{-\beta y}\right)e^{int} + \left[\frac{\alpha^2Re^2}{\pi-\lambda}\left[e^{-\lambda y}\left(\frac{\pi}{2\lambda\alpha Re}e^{-(\lambda-\alpha Re)y} - \frac{\lambda}{\pi\alpha Re}e^{-(\pi-\alpha Re)y}\right)\right]\right.\right.\\
\left.\left. + K\left[\begin{array}{c} Fe^{-\lambda y} + (A-C)e^{-(\lambda-\alpha Re)y} + \\ (D-B+Ey)e^{-(\pi-\alpha Re)y} - 2Eye^{-(\lambda-\alpha Re)y}\end{array}\right]\right]\cos\,\pi z\right].
\end{aligned} \tag{45}$$

6. Shear Stress Components

Shear stress components in $x-$ and $z-$ directions, respectively, are

$$C_{f_x} = \frac{(\partial u/\partial y)_{y=0}}{\alpha Re}, \tag{46}$$

or

$$\begin{aligned}
C_{f_x} = -1 + K(\alpha Re)^2 + \epsilon\frac{\beta e^{int}}{\alpha Re} + \epsilon\left[-\left[\left(\frac{\lambda}{\pi}-\frac{\pi}{2\lambda}\right) + \left(\frac{\pi(\alpha Re-\lambda)}{2\lambda} - \frac{\lambda(\alpha Re-\pi)}{\pi}\right)\right]\frac{\lambda}{\pi-\lambda}\right.\\
\left. + \frac{\epsilon K}{\alpha Re}\left[\begin{array}{c} -\lambda(-A+B+C-D) + (A-C)(\alpha Re-\lambda) \\ +(D-B)(\alpha Re-\pi) - E\end{array}\right]\right],
\end{aligned} \tag{47}$$

and

$$C_{f_z} = \frac{\mu(\partial w/\partial y)_{y=0}}{\alpha}, \tag{48}$$

or

$$C_{f_z} = \mu\lambda \sin \pi z. \tag{49}$$

7. Results and Discussions

In the present study, a 3-dimensional transient flow of a second grade fluid over a porous plane having periodic suction and time dependent free stream velocity is modeled and analyzed theoretically. Analytic expressions for the velocity field, pressure, and skin friction are computed by the perturbation technique. On these physical quantities, the effects of *Re* (Reynolds number), *K* (elastic parameter), *a* (suction parameter), *t* (time parameter), and *n* (frequency parameter) are visualized graphically. For the sake of the physical inside into the problem, the velocity field, skin friction components, and pressure are conferred by passing on numerical values to numerous nondimensional parameters arising in the mathematical model of the problem.

Figure 1 displays the effect of *Re, n, t*, suction parameter *a,* and elastic parameter *K* on the transient velocity *u.* In Figures 1(a)–1(e), one of the parameters varies while all other nondimensional parameters are fixed. In Figure 1(a), $Re = 8, 10, 15$, whereas other parameters are fixed i. e., $t = 0.5$, $a = -0.1$, $n = 5$, $z = 0$, $K = 0.05$, and $\varepsilon = 0.05$. It is detected that with the upsurge of the *Re*, the velocity component *u* also upsurges and grasps its maximum value at the boundary for each value of the *Re* is taken in this regard. Physically it meant that inertial forces are overriding the viscous forces. Moreover, the boundary layer thickness declines with a growth in *Re*. Similarly, it is perceived that the velocity component *u* (Figure 1(b)) increases with a rise in *n.* This upshot is very effective in the vicinity of the plate. Also, this is motivating to note that all velocity profiles tend to unity, away from the plate. Figure 1(c) displays the influence of the transient number on *u*. It discloses that an upsurge in time parameter results in a reduction in *u.* This is quite in agreement with the physical fact that unsteady flow approaches to steady flow after large time. It is evident that *u* (Figure 1(d)) rises with a growth in suction parameter *a*. In general, a rise in *a* leads to decelerate the flow velocity. Of course, in this case, an enhancement in *u* is because of the transient free stream velocity. Figure 1(e) parades the impact of *K* on *u*. It is detected that a growth in *K* leads to a reduction in *u*, which looks correct physically as an increase in *K* results in fluid thickening causing reduction in the velocity.

Impact of Reynolds number *Re,* frequency parameter *n,* time parameter *t*, suction parameter α, and elastic parameter *K* on *u* is presented in Figure 2 for *z* as abscissa. It is observed that a growth in *Re* (Figure 2(a)) leads to enhance the amplitude of oscillation and consequently enhancement in main flow which is in agreement with the results discussed in the Figure 1(a). The similar behavior is noted for the suction parameter on *u* (Figure 2(d)). It is seen from Figure 2(b) that enhancement in the values of *n* only shifts the location of oscillation. Similar impact of *t* on *u* is noted (Figure 2(c)). It is examined from Figure 2(e) that larger value of *k* rises the amplitude of oscillation.

Figure 3 illustrates the impact of *Re* and α on *v* and *w*. The magnitude of *v* shrinks with a growth in *Re* (Figure 3(a)). Instead, magnitude of *v* increases for growing values of α, and this influence is significant near the plate (Figure 3(c)), and it appears physically true, since it is well known that the suction impact on the flow is maximum adjacent to the plate. Further, the velocity component *v* becomes stable as $y \longrightarrow \infty$. It is detected from Figure 3(b) that for a fixed value of *Re*, *w* rises exponentially adjacent to the plate, achieves its maximum value, and then declines rapidly, and ultimately approaches to 0 as $y \longrightarrow \infty$. Adjacent to the plate, a parabolic profile is attained. This velocity component growths with a rise in *Re* adjacent to the plate but possesses opposite trend away from the plate. Physically, it reflects the dominance of inertial forces over viscous forces adjacent to the plate. However, away from the plate, viscous forces dominate the inertial forces due to oscillatory free steam velocity resulting opposite trend of velocity component *w* and eventually approaching to zero far away from the plate. It is viewed from Figure 3(d) that, for a fixed value of *a*, *w* growths exponentially adjacent to the plate, achieves its optimum (maximum value), then shrinkages rapidly, and lastly approaches to zero as $y \longrightarrow \infty$. Adjacent to the plate, a parabolic profile is attained. It is also observed that the suction parameter enhances the velocity component near the plate which is against the general conception (suction parameter leads to decelerate velocity). An enhancement, in fact, in the velocity component near the plate is because of the transient free stream velocity.

Figure 4 exemplifies the impact of *Re* and α on *v* and *w* against *z* as abscissa. It is perceived from Figure 4(a) that an increase in *Re* causes a decline in the amplitude of oscillation resulting reduction in the flow velocity in the $y-$ direction. Further, the impact of *Re* on *w* (Figure 4(b)) is to upsurge the amplitude of oscillation and consequently enhancement in velocity component *w* agree with the results discussed previously (Figure 3(b)). From Figure 4(d), similar influence of α on *w* is noted. The behavior of α on *v* is shown in Figure 4(c). It is found that increasing α just results in shift of the axis of oscillation.

Figure 5 displays the effect *Re*,α, and *K* on the pressure. In Figure 5(a), Reynolds number is varied, that is, $Re = 8, 10, 15$ and other existing parameters are fixed, i. e., $\alpha = -0.1, z = 0$, $K = 0.05$, and $\varepsilon = 0.05$. The pressure grows near the plate with the rise in *Re.* It shows the dominance of inertial forces over the viscous forces. Of course, the pressure attains a steady value far away from the plate. In contrast, the impact of α is to decline the pressure near the plate (Figure 5(b)). Moreover, pressure converges to a steady value away from vicinity of the plate, where the suction effect vanishes, for increasing values of suction parameter. From Figure 5(c), it is perceived that the pressure decreases adjacent to the plate when *K* is elevated. It is consistent with the

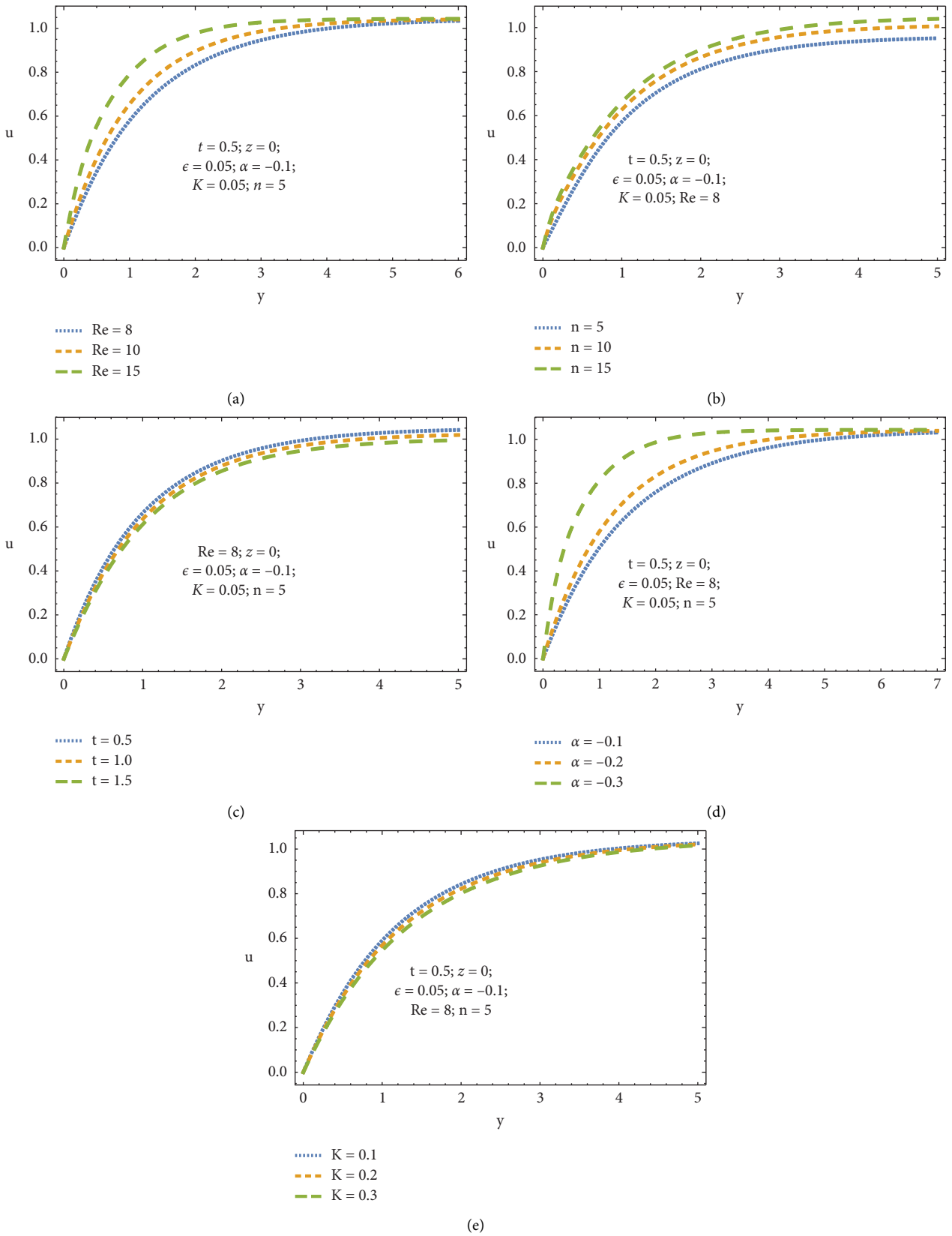

FIGURE 1: Impact of all nondimensional parameters on main flow. (a) Impact of Re on u. (b) Impact of n on u. (c) Impact of t on u. (d) Impact of α on u. (e) Impact of K on u.

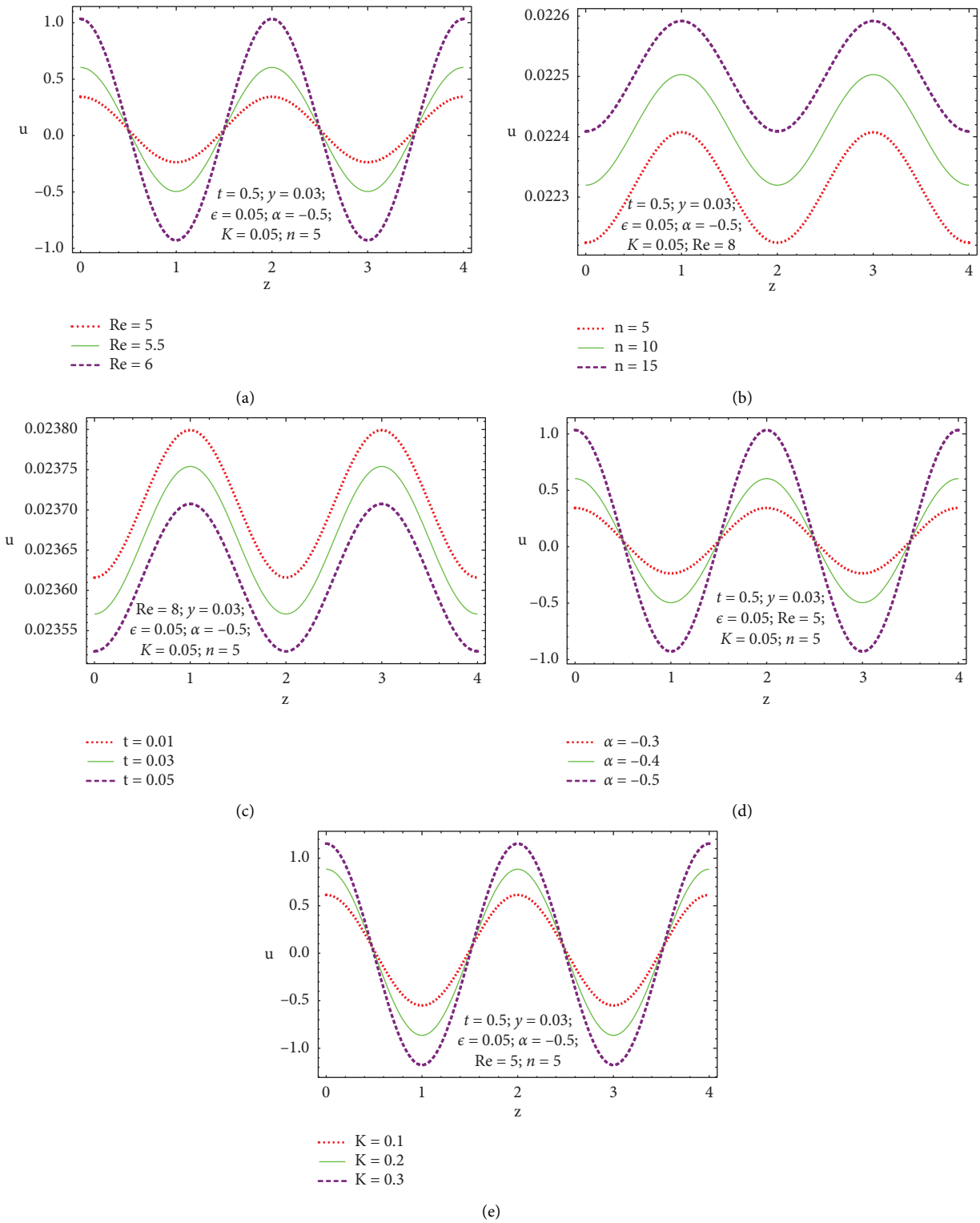

FIGURE 2: Impact of nondimensional parameters on main flow for **z** as abscissa. (a) Impact of *Re* on *u*. (b) Impact of *n* on *u*. (c) Impact of *t* on *u*. (d) Impact of α on *u*. (e) Impact of *K* on *u*.

physical result that the boundary layer is thinned by suction causing reduction in pressure near the plate. Further, similar to influence of α on the pressure far away from the plate, pressure again approaches to a steady value away from vicinity of the plate for increasing values of *K*.

Figure 6 characterizes the impact of *Re*,α, and *K* on pressure against *z* as abscissa. It is perceived from Figure 6(a) that growth in *Re* results in enhancement in the amplitude of oscillation causing a rise in the pressure. Similar effect of α (Figure 6(b)) and *K* (Figure 6(c)) on the pressure is found.

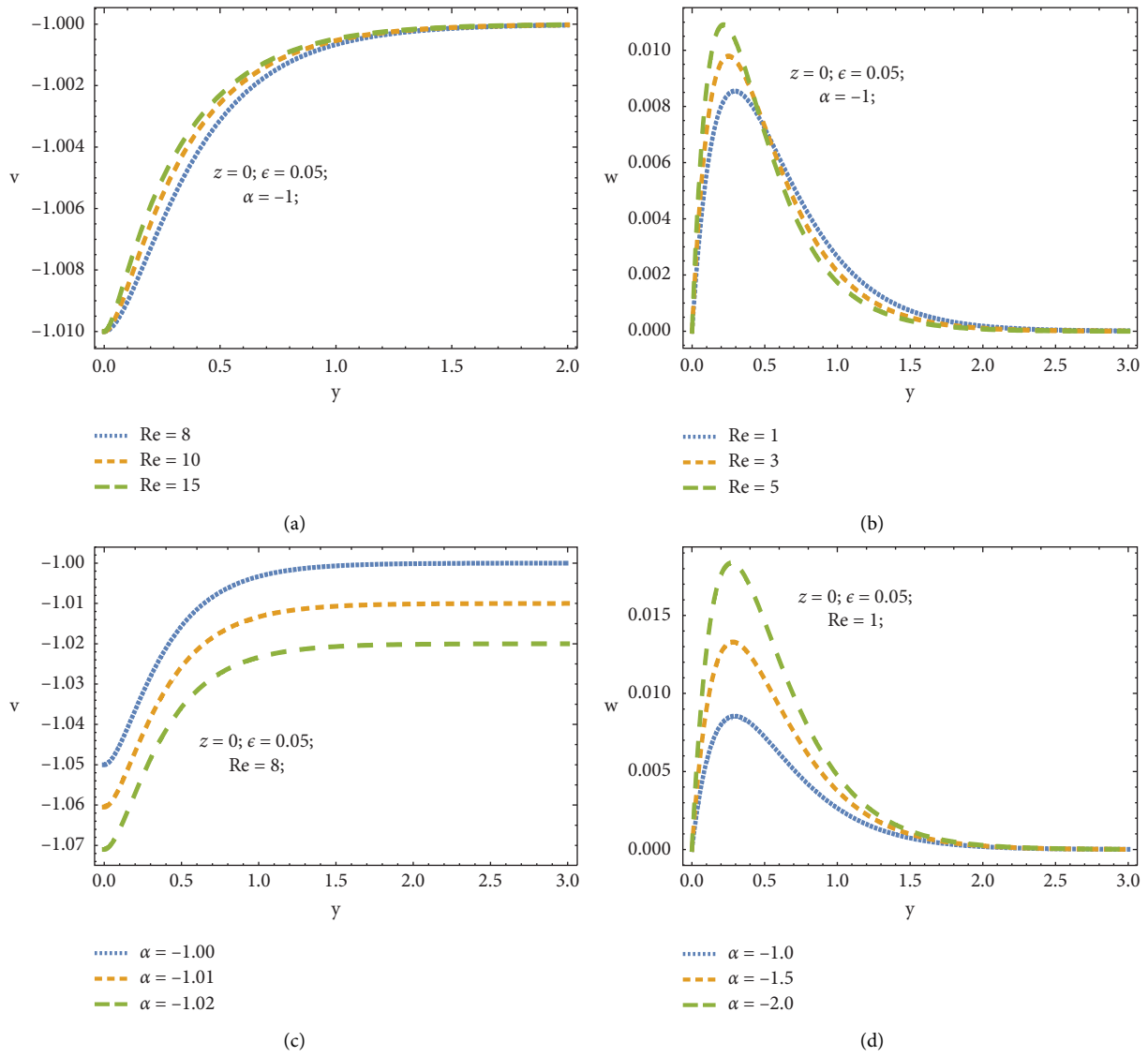

FIGURE 3: Impact of nondimensional parameters on v and w. (a) Impact of Re on v (b) Impact of Re on w. (c) Impact of α on v. (d) Impact of α on w.

Figure 7 typifies C_{f_x} (nondimensional skin friction component) in the main flow direction against Re for numerous values of frequency parameter n, transient number t, a, and K. Figure 7(a) shows the growing influence on C_{f_x} magnitude for increasing values of n. It is also revealed that there is exponential falloff in the magnitude of this skin friction component for $0.5 \le Re \le 1.5$ up to a certain value depending upon the value of n taken in this regard and then a rapid rise in the magnitude of this friction component is observed. Physically it reflects the dominance role of viscous forces over inertial forces for the range $0.5 \le Re \le 1.5$. Of course, it is worthwhile to point out that the role of viscous forces over inertial forces is overturned when $Re > 1.5$. On the contrary, the role of t regarding its impact on C_{f_x} is inverted (Figure 7(b)). Figure 7(c) portrays the effect of α upon C_{f_x}. It is observed that the magnitude of C_{f_x} decreases for $0.5 \le Re \le 1.4$ and then increases exponentially for rising values of α. It shows the dominant role of viscous forces over the inertial forces in the range $0.5 \le Re \le 1.4$ causing decay in C_{f_x} magnitude. In contrast, for $Re > 1.4$, inertial forces overcome the viscous forces resulting rapid grow in C_{f_x} magnitude. In Figure 7(d), similar behavior of K on C_{f_x} is noted for $Re > 1.1$, and increasing values of K has no significant impact for $0.5 \le Re \le 1.1$.

Figure 8 is traced for C_{f_z} (nondimensional skin friction component) in the z-direction versus Re for various values of K and α. It is detected that a growth in Re results in growth in C_{f_z} magnitude in both cases. Further, the enhancement in C_{f_z} magnitude by increasing suction parameter (Figure 8(a)) seems naturally correct as the role of suction is to promote the resistance in flow causing growth in the skin friction. It is also detected that increasing elastic parameter results

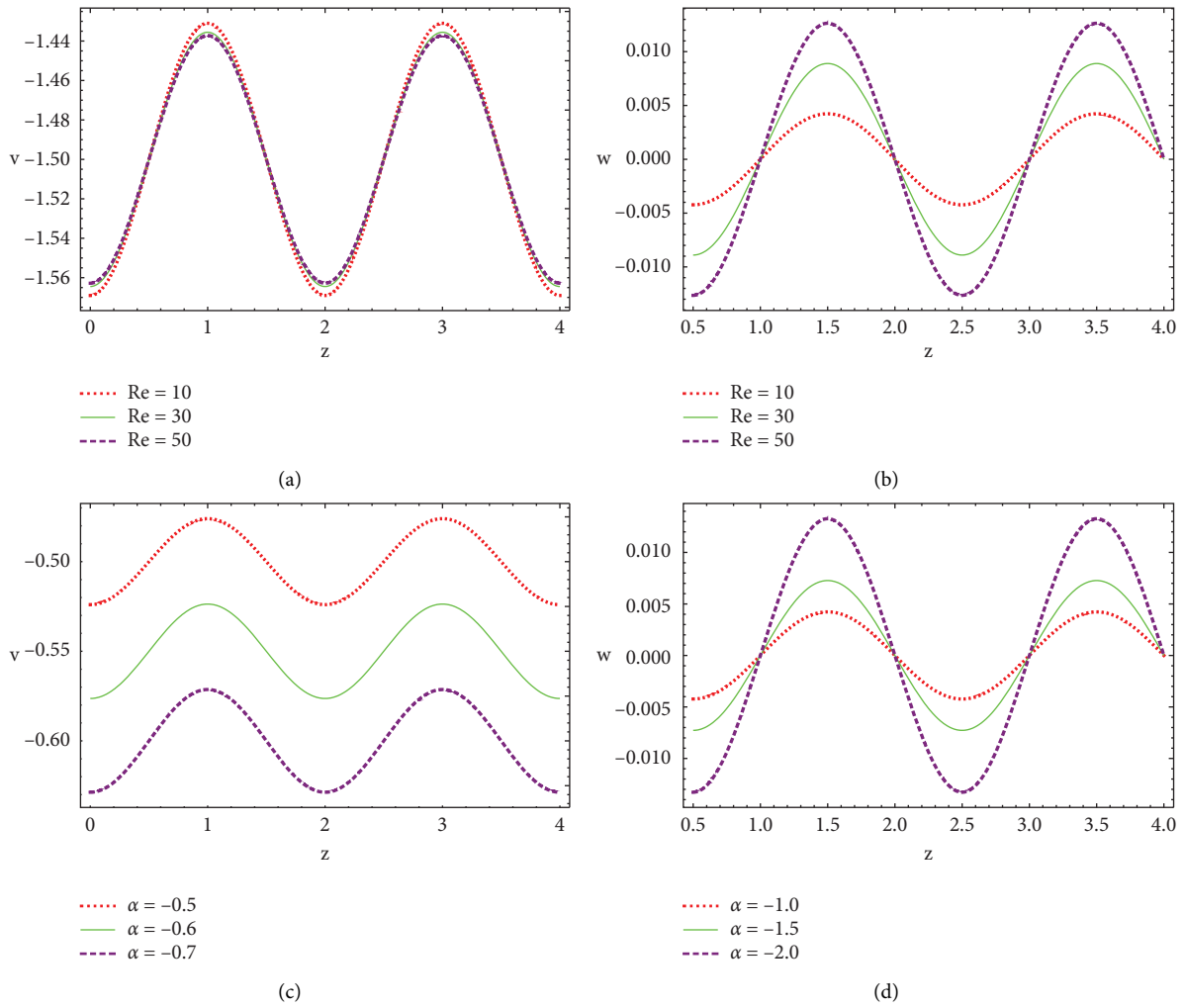

FIGURE 4: Impact of nondimensional parameters on v and w for z as abscissa. (a) Impact of Re on v. (b) Impact of Re on w. (c) Impact of α on v. (d) Impact of α on w.

(Figure 8(b)) in escalation of skin friction magnitude. In fact, an increase in K results in the thickening of fluid causing rise in skin friction.

8. Remarks

This analysis aims to explore analytic solutions for 3-dimensional fluctuating flow of a second grade fluid with periodic suction. Approximate solutions for u, v, w (velocity field), C_x, C_{f_z} (skin friction components), and pressure based upon perturbation are computed and explored theoretically. As a regular perturbation technique based upon small parameter existing in the governing equations, series solutions obtained by this method always converges. Consequently, analytic solutions for u, v, w computed by this approach in this work also converges. The conclusions of this analysis are as follows:

(i) Velocity component u grows with Re, frequency parameter n and α, whereas it declines with increasing time parameter and non-Newtonian parameter

(ii) v increases with growing values of Re, and it decreases for growing values of α, and this impact is significant near the plate and ultimately it becomes stable as $y \longrightarrow \infty$

(iii) w is noted to be enhancing exponentially adjacent to the plate, attaining its optimum (maximum) value, then decreasing rapidly, and ultimately approaches to 0 as $y \longrightarrow \infty$ due to Re and α

(iv) A rise in Re, n, a, and K leads to enhance the oscillation amplitude and consequently enhancement in u whereas enhancement in transient parameter causes an inverse effect

(v) The amplitude of oscillation of cross flow velocity w upsurges due to enhancement in Re and α causing intensification in the flow velocity. In contrast, Re possesses inverse impact on cross flow velocity v

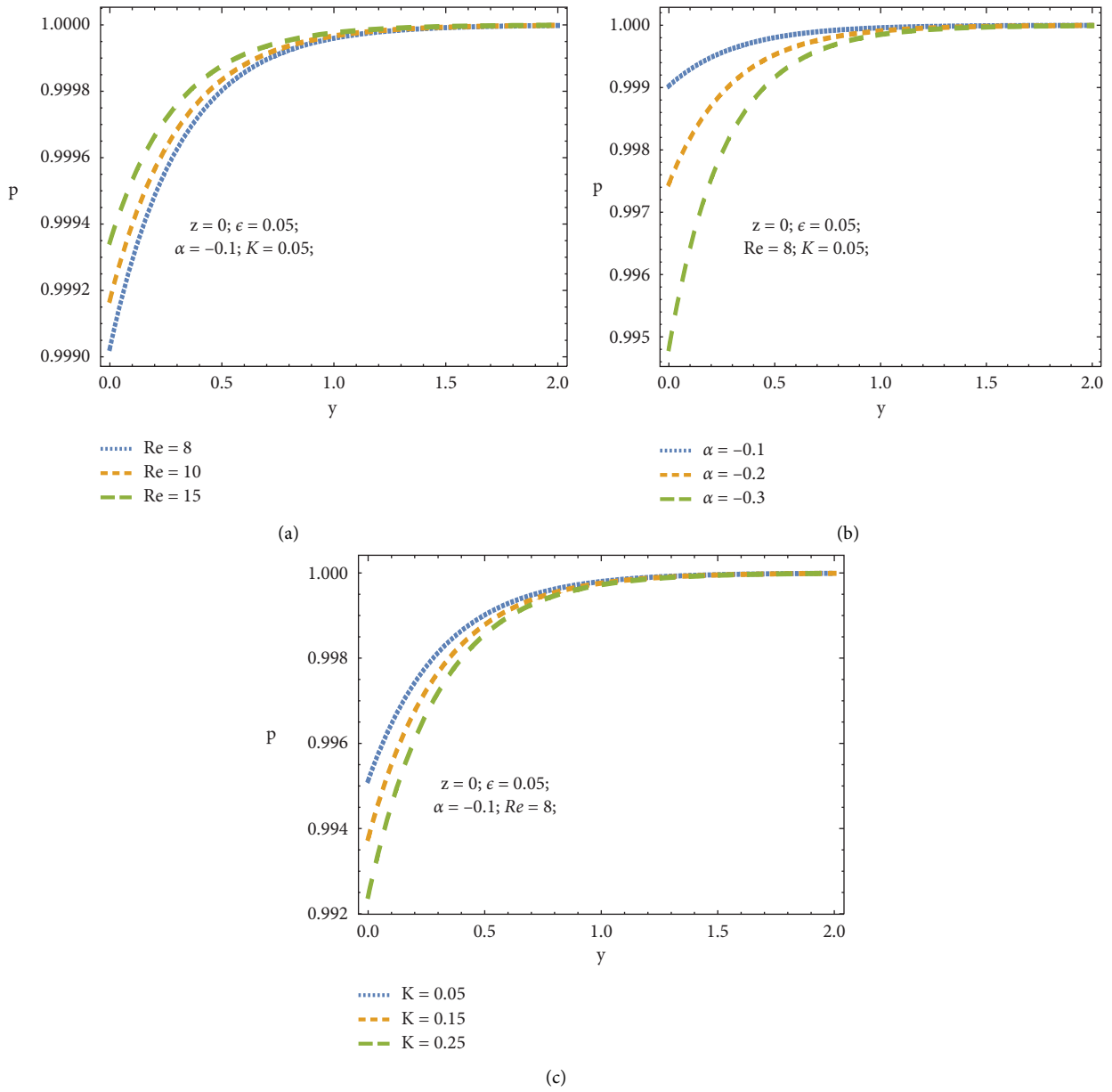

Figure 5: Impact of nondimensional parameters on pressure. (a) Impact of Re on p. (b) Impact of α on p. (c) Impact of K on p.

(vi) The influence of Re is to boost the pressure; however, α and K possess inverse impact on it

(vii) The effect of suction parameter α and non-Newtonian parameter K is to decrease the pressure near the plate

(viii) The growth in Re,α, and K results in enhancement in the amplitude of oscillation causing rise in the pressure

(ix) C_{f_x} rises for growing values of n, and the role of t regarding its impact on C_{f_x} is inverted

(x) It is observed that C_{f_x} decreases for $0.5 \leq Re \leq 1.4$ and then increases exponentially for rising values of α and K

(xi) The role of viscous forces over the inertial forces is found to be dominant for $0.5 \leq Re \leq 1.4$; in contrast, this role is noted to be inverted for $Re > 1.4$

(xii) C_{f_z} enhances for rising values α,K, and Re

(xiii) A growth in Re causes to decline boundary layer thickness

(xiv) Inertial forces are found to be dominant over viscous forces adjacent to the plate

(xv) Results of [11] are recovered for non-Newtonian parameter $K \longrightarrow 0$

(xvi) Results of Ref. [21] are validated under identical physical conditions

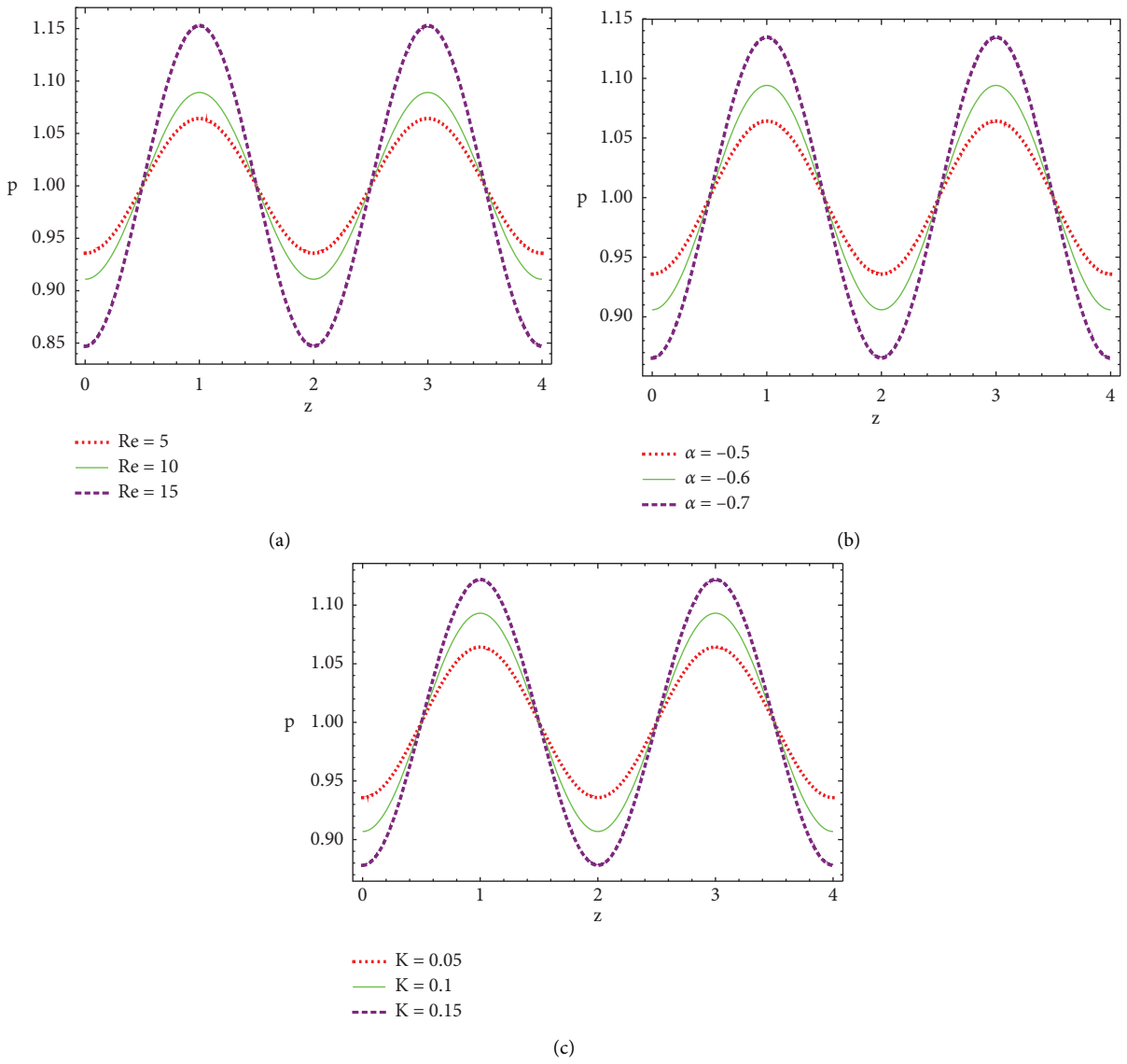

FIGURE 6: Impact of nondimensional parameters on pressure for **z** as abscissa. (a) Impact of Re on p. (b) Impact of α on p. (c) Impact of K on p.

Abbreviations

English Letters

$\widetilde{A}_1, \widetilde{A}_2$: Rivlin–Erickson tensors
A_1: Constants of integrations
C_{f_x}: Shear stress along the x-direction (N/m^2)
C_{f_z}: Shear stress along the z-direction (N/m^2)
$\widetilde{I}$: Identity tensor
l: Half-wave length of the periodic suction velocity (m)
p and p_∞: Pressure and constant pressure (N/m^2)
T: Time (s)
n: Frequency parameter (Hz)
K: Elastic parameter for the second-grade fluid (dimensionless)
Re: Reynolds number (dimensionless)
U_0: Mean constant free stream velocity (m/s)
V_0: Mean constant suction velocity (m/s)
u, v, w: Components of velocity in $x-, y-, z-$ directions (m/s)

Greek Letters

α: Suction parameter
α_1, α_2: Material constants (kg/m)
ρ: Fluid density (kg/m^3)
ϵ: Small reference parameter (amplitude)
μ: Coefficient of viscosity (kg/ms)
ϑ: Kinematic viscosity (m^2/s)
$\widetilde{\tau}$: Cauchy stress tensor
∇: Gradient operator $(1/m)$.

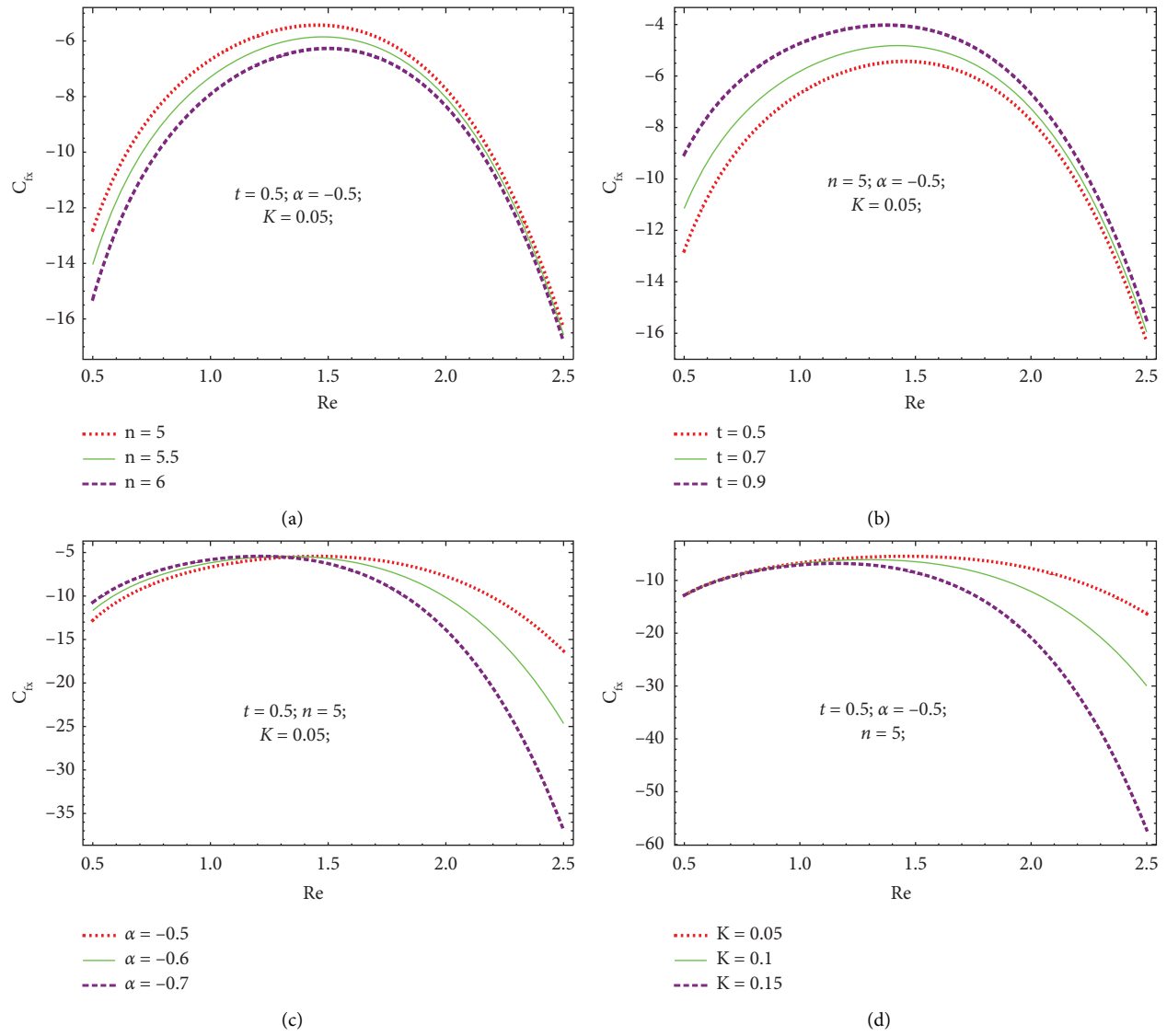

Figure 7: Impact of nondimensional parameters on skin friction the along x-axis. (a) Impact of n on skin friction along the x-axis. (b) Impact of t on skin friction along the x-axis. (c) Impact of α on skin friction along the x-axis. (d) Impact of K on skin friction along the x-axis.

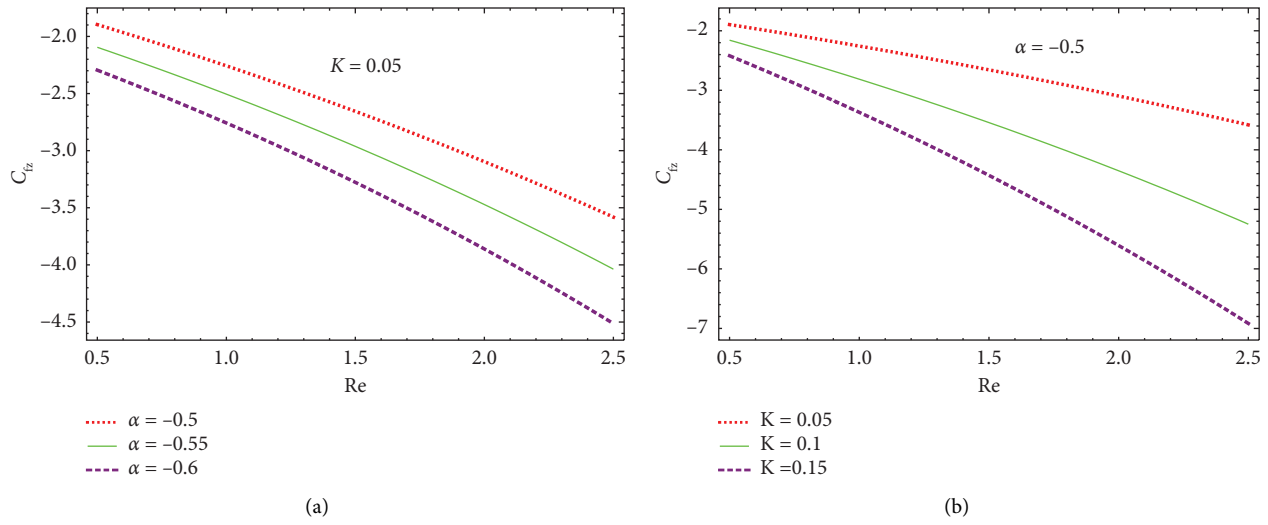

Figure 8: Impact of nondimensional parameters on skin friction the along the z-axis. (a) Impact of α on skin friction along the z-axis. (b) Impact of K on skin friction along the z-axis.

Data Availability

No data were used to support this study.

Additional Points

Various non-Newtonian fluid models such as Jeffery, Maxwell, Oldroyd-B, etc. (both isothermal and non-isothermal) are favourite models for future work. Applicability: (Aeronautical Engineering) Designing and manufacturing laminar flow control system (LFCS) to enhance the vehicle power requirement.

Conflicts of Interest

The authors declare that there are no conflicts of interest.

Authors' Contributions

M. A. Rana originated the idea of the problem and physics of effect of nondimensional parameters. Reviewed and revised the manuscript. Mehwish Zafar implemented the idea by embedding it into mathematical model and solution methodology and wrote the manuscript thoroughly. Atifa Latif developed mathematical code for graphs and prepared all the graphs.mmc1.

References

[1] G. V. Lachmann, "Boundary layer and flow control," *Its Principles and Applications*, Pergamon Press, Oxford, United Kingdom, 1961.

[2] M. J. Lighthill, "The response of laminar skin-friction and heat transfer to fluctuations in the stream velocity," *Proc. Roy. Soc., Sec. A*, vol. 224, pp. 1–23, 1954.

[3] J. T. Stuart, "Two-dimensional flow past an infinite, porous plate with constant suction and periodic free stream," *Proc. Royal Soc*, vol. 231A, p. 116, 1955.

[4] S. A. S. Messiha, "Laminar boundary layers in oscillatory flow along an infinite flat plate with variable suction," *Mathematical Proceedings of the Cambridge Philosophical Society*, vol. 62, no. 2, pp. 329–337, 1966.

[5] V. M. Soundalgekar, "Free convection effects on the flow past an infinite vertical oscillating plate," *Astrophysics and Space Science*, vol. 64, no. 1, pp. 165–171, 1979.

[6] A. Raptis, "Unsteady free convective flow through a porous medium," *International Journal of Engineering Science*, vol. 21, no. 4, pp. 345–348, 1983.

[7] K. D. Singh and S. K. Rana, "Three-dimensional flow and heat transfer through a porous medium," *Indian Journal of Pure and Applied Mathematics*, vol. 23, pp. 905–914, 1992.

[8] K. D. Singh, "Three dimensional oscillatory flow in a porous medium," *Proc. Indian natn. Sci. Acad*, vol. 58A, no. 2, pp. 125–132, 1992.

[9] K. A. Helmy, "On the flow of an electrically conducting fluid and heat transfer along a plane wall with periodic suction," *Meccanica*, vol. 28, no. 3, pp. 227–232, 1993.

[10] M. Guria and R. N. Jana, "Three-dimensional fluctuating Couette flow through the porous plates with heat transfer," *International Journal of Mathematics and Mathematical Sciences*, vol. 2006, Article ID 61023, 18 pages, 2006.

[11] S. Ahmed, "The effect of viscous dissipative heat on three dimensional oscillatory flow with periodic suction velocity," *Indian Journal of Science and Technology*, vol. 3, no. 3, pp. 276–283, 2010.

[12] S. Ahmed, "Transient three dimensional flows through a porous medium with transverse permeability oscillating with time," *Emirates Journal for Engineering Research*, vol. 13, no. 3, pp. 11–17, 2008.

[13] S. Ahmed, "Oscillatory three dimensional flow and heat and mass transfer through a porous medium in presence of periodic suction," *Emirates Journal for Engineering Research*, vol. 15, no. 2, pp. 49–61, 2010.

[14] W. K. Hasan and M. A. Mahmood, "Transient Three-dimensional natural convection in confined porous media with time-periodic boundary conditions," *Journal of Al Rafidain University College*, vol. 32, pp. 199–231, 2013.

[15] K. Gersten and J. F. Gross, "Flow and heat transfer along a plane wall with periodic suction," *Journal of Applied Mathematics and Physics*, vol. 25, no. 3, pp. 399–408, 1974.

[16] P. Puri, "Fluctuating flow of a viscous fluid on a porous plate in a rotating medium," *Acta Mechanica*, vol. 21, no. 1-2, pp. 153–158, 1975.

[17] S. S. Chawla, "Fluctuating flow induced by periodic suction through a rotating disk," *Acta Mechanica*, vol. 25, no. 3-4, pp. 207–219, 1977.

[18] R. N. Jana and N. Datta, "Effect of rotation on the flow past a porous plate with time-dependent free stream," *Zeitschrift fur Flugwissenschaften und Weltraumforschung*, vol. 3, pp. 241–245, 1979.

[19] F. Mabood, A. Shafiq, T. Hayat, and S. Abelman, "Radiation effects on stagnation point flow with melting heat transfer and second order slip," *Results in Physics*, vol. 7, no. 2017, pp. 31–42, 2017.

[20] M. Shoaib, A. M. Siddiqui, M. A. Rana, and A. Imran, "Three-dimensional flow of a second grade fluid along an infinite horizontal plane wall with periodic suction," *American Scientific Research Journal for Engineering, Technology, and Sciences (ASRJETS)*, vol. 18, no. 1, pp. 153–170, 2016.

[21] M. A. Rana and A. Latif, "Three-dimensional free convective flow of a second-grade fluid through a porous medium with periodic permeability and heat transfer," *Boundary Value Problems*, vol. 2019, no. 1, 44 pages, 2019.

[22] M. M. Bhatti, A. Zeeshan, F. Bashir, S. M. Sait, and R. Ellahi, "Sinusoidal motion of small particles through a Darcy-Brinkman-Forchheimer microchannel filled with non-Newtonian fluid under electro-osmotic forces," *Journal of Taibah University for Science*, vol. 15, no. 1, pp. 514–529, 2021.

[23] A. Riaz, A. Zeeshan, S. Ahmad, A. Razaq, and M. Zubair, "Effects of external magnetic field on non-Newtonian two phase fluid in an annulus with peristaltic pumping," *Journal of Magnetics*, vol. 24, no. 1, pp. 62–69, 2019.

[24] B. J. Gireesha, R. S. R. Gorla, and B. Mahanthesh, "Effect of suspended nanoparticles on three-dimensional MHD flow, heat and mass transfer of radiating Eyring-Powell fluid over a stretching sheet," *Journal of Nanofluids*, vol. 4, no. 4, pp. 474–484, 2015.

[25] B. Mahanthesh, B. J. Gireesha, and R. S. R. Gorla, "Nonlinear radiative heat transfer in MHD three-dimensional flow of water based nanofluid over a non-linearly stretching sheet with convective boundary condition," *Journal of the Nigerian Mathematical Society*, vol. 35, no. 1, pp. 178–198, 2016.

[26] A. Shafiq, G. Rasool, C. M. Khalique, and S. Aslam, "Second grade bioconvective nanofluid flow with buoyancy effect and chemical reaction," *Symmetry*, vol. 12, no. 4, pp. 621–718, 2020.

[27] F. Mabood, M. D. Shamshuddin, and S. R. Mishra, "Characteristics of thermophoresis and Brownian motion on radiative reactive micropolar fluid flow towards continuously moving flat plate: HAM solution," *Mathematics and Computers in Simulation*, vol. 191, no. 2022, pp. 187–202, 2022.

[28] M. D. Shamshuddin, F. Mebarek-Oudina, S. O. Salawu, and A. Shafiq, "Thermophoretic movement transport of reactive Casson nanofluid on Riga plate surface with nonlinear thermal radiation and uneven heat sink/source," *Journal of Nanofluids*, vol. 11, no. 6, pp. 833–844, 2022.

[29] R. P. Chhabra and J. F. Richardson, *Non-Newtonian Flow and Applied Rheology: Engineering Applications*, Elsevier, Amsterdam, Netherlands, 2008.

[30] F. Irgens, *Rheology and Non-newtonian Fluids*, Springer International Publishing, Switzerland, 2014.

[31] J. E. Dunn and R. L. Fosdick, "Thermodynamics, stability, and boundedness of fluids of complexity 2 and fluids of second grade," *Archive for Rational Mechanics and Analysis*, vol. 56, no. 3, pp. 191–252, 1974.